Catalysis Communications 159 (2021) 106342

Contents lists available at ScienceDirect

Catalysis Communications

journal homepage: www.elsevier.com/locate/catcom

Short communication

Combustion method combined with sonochemical step for synthesis of maghemite-supported catalysts for the hydrogenation of 2,4-dinitrotoluene

Viktória Hajdu [a], Gábor Muránszky [a], Masahiro Hashimoto [b], Ferenc Kristály [c], Milán Szőri [a], Béla Fiser [a], Zoltán Kónya [d], Béla Viskolcz [a], László Vanyorek [a,*]

[a] Institute of Chemistry, University of Miskolc, Miskolc-Egyetemváros, 3515, Hungary
[b] JEOL (EUROPE)SAS 1, Allée de Giverny, 78290 Croissy-Sur-Seine, France
[c] Institute of Mineralogy and Geology, University of Miskolc, Miskolc-Egyetemváros, 3515, Hungary
[d] University of Szeged, Department of Applied and Environmental Chemistry, 6720 Szeged, Rerrich Béla Square 1, Hungary

ARTICLE INFO

Keywords:
Toluenediamine
Maghemite
Sonochemistry
Catalyst
Hydrogenation

ABSTRACT

Maghemite particles were synthesized by using a combined combustion method and sonochemical step. Maghemite was used as carrier to prepare supported Pt and Pd catalysts after deposition via a sonochemical step. The catalysts were immediately ready to be used (metals were catalytically active) for the 2,4-dinitrotoluene hydrogenation to produce 2,4-toluenediamine. The most active catalysts were the Pd/maghemite and bimetallic Pd-Pt/maghemite. The catalysts were easily separable after reaction due to their magnetic properties.

1. Introduction

The hydrogenation of 2,4-dinitrotoluene (DNT) is an important industrial process to produce 2,4-toluelendiamine (TDA). TDA is an intermediate in the production of toluene diisocyanate (TDI), which is one of the main components in the manufacture of polyurethane (PU) [1]. In the catalytic hydrogenation of DNT, carbon-, silica- and alumina-supported transition metals (Pd, Pt, Ni, etc.) or transition metal oxides are the most commonly used catalysts [2–8]. Many intermediates can be formed during the process, such as 4-(hydroxyamino)-2-nitrotoluene (4HA2NT), 2-(hydroxyamino)-4-nitrotoluene (2HA4NT), 4-amino-2-nitrotoluene (4A2NT) and 2-amino-4-nitrotoluene (2A4NT) [9–11]. The best catalysts have high catalytic activity, it is easy to use them, and their recovery is excellent. However, it is difficult to separate powder catalysts (such as supported-activated carbon) from the reaction medium due to their stable dispersion forming ability. The use of magnetic nanoparticles might be a solution to this problem, because the small, mobile particles can be easily removed and isolated by a magnetic field. This simplifies the catalyst recovery and recyclability [12], and by avoiding conventional filtration and centrifugation methods, the associated catalyst loss is also eliminated. Therefore, the use of magnetic nano-catalysts is a promising alternative, especially in heterogeneous catalysis. One of the most widely used magnetic material is maghemite [13,14]. Various methods have been applied to synthesize maghemite nanoparticles, such as sol-gel synthesis [15,16], microemulsion [17,18], coprecipitation [19,20], hydrothermal [21], flow injection [22], and combustion methods [23]. However, the overall process usually includes several steps, and post-treatment to activate the catalysts is also required. Therefore, attempts to simplify the catalyst production process were made and a new method has been developed in our research group [24,25]. By using this method, an active catalyst has been developed during the impregnation step [24,25]. The essence of the method is the exposure of the liquid medium to intense ultrasonic effects, where the induced sound waves create cycles of high and low pressure. Thus, the vapor pressure of the solvent is decreasing momentarily, which results in the formation of bubbles of a few micrometers in size in the mixture. These bubbles are pulsating and growing until they reach a higher pressure range in the liquid, where they collapse as the pressure increases [26]. At this point ("hot spot"), a large amount of energy is released, causing the medium to act as reducing agent in the reaction and to initiate the formation of metal, metal oxide, or metal hydroxide solid particles [27–32]. By using our recently developed sonochemical method, in this work palladium and platinum nanoparticles were deposited on the surface of maghemite and tested in the catalytic DNT hydrogenation reaction.

* Corresponding author.
E-mail address: kemvanyi@uni-miskolc.hu (L. Vanyorek).

https://doi.org/10.1016/j.catcom.2021.106342
Received 19 April 2021; Received in revised form 26 July 2021; Accepted 28 July 2021
Available online 29 July 2021
1566-7367/© 2021 Published by Elsevier B.V. This is an open access article under the CC BY-NC-ND license (http://creativecommons.org/licenses/by-nc-nd/4.0/).

2. Experimental

2.1. Materials

Iron(III) citrate hydrate ($FeC_6H_5O_7$ x H_2O, PanReac AppliChem Ltd) and polyethylene glycol with 400 g/mol molar mass (PEG400, Sigma Aldrich Ltd) were used for the production of maghemite nanopowder. Palladium(II) nitrate dihydrate ($Pd(NO_3)_2$ x $2H_2O$, Merck Ltd), hydrogen hexachloroplatinate (H_2PtCl_6, Reanal Ltd), hydrazine hydrate (N_2H_4 x H_2O, Sigma Aldrich Ltd) and patosolv (a mixture of 90 vol% ethanol and 10 vol% isopropanol, Molar Chem. Ltd) were used to provide the palladium and/or platinum content of the metal supported maghemite catalysts.

2,4-dinitrotoluene (DNT, $C_7H_6N_2O_4$) was used as reactant, and 2,4-diaminotolune ($C_7H_{10}N_2$), 2-methyl-5-nitroaniline, 2-methyl-3-nitroaniline, 4-methyl-3-nitroaniline, and 4-methyl-2-nitroaniline ($C_7H_8N_2O_2$) were used as standards (Sigma Aldrich Ltd) for the GC–MS measurements during the catalytic tests. Methanol (CH_3OH) was used as solvent (Merck Ltd) during these measurements.

2.2. Catalysts characterization methods

The maghemite nanoparticles and the palladium decorated maghemite were examined by high-resolution transmission electron microscopy (HRTEM, FEI Technai G2 electron microscope, 200 kV). During the preparation step, drops of the aqueous suspension of samples were placed onto copper grids (Ted Pella Inc., only carbon, 300 mesh). The size of the nanoparticles was estimated based on the HRTEM images and the original scale bar by using the ImageJ software. Powder X-ray diffraction (XRD) measurements were conducted by using a Rigaku Miniflex II diffractometer with CuKα radiation source (30 kV, 15 mA). To identify the functional groups on the surface of the maghemite nanopowder, a Bruker Vertex 70 Fourier transform infrared spectrometer (FTIR) was used. The prepared maghemite (2 mg) was added to 250 mg spectroscopic potassium bromide, and after homogenization a pellet was formed which was used in the measurements.

Specific surface area (SSA, m^2/g) of the catalysts was determined by nitrogen adsorption-desorption measurements at 77 K using a Micromeritics ASAP 2020 sorptometer and based on the Brauner-Emmett-Teller (BET) method. The carbon content of the maghemite was measured by Vario Macro CHNS element analyser equipment, and phenanthrene was used as standard (C: 93.538%, H: 5.629%, N:0.179%, S: 0.453%; Carlo Erba Inc). The carrier gas used was He (99.9990%), while O_2 (99.995%) was used for oxidation, and the samples were loaded onto tin foils.

2.3. Preparation of maghemite-supported palladium and platinum catalysts

A recently developed combined method [24,25] which includes combustion and sonochemical steps was applied to synthesize maghemite nanoparticles (Fig. S1, first two steps). In the first step, 7.0 g iron (III) citrate hydrate was dispersed in 40.0 g polyethylene glycol (PEG 400) by using a Hielscher UIP1000Hdt ultrasound tip homogenizer for 5 min (20 kHz). The colour of the PEG 400-based dispersion changed to red, which indicated that iron oxyhydroxide (ferrihydrite and goethite) colloid has formed. In the second step, the pegylated iron oxyhydroxide dispersion was heated up and the organic compound was burned. Thus, magnetic nanopowder (mainly maghemite) was formed.

Palladium nitrate (0.25 g) was solved in 50 mL patosolv, and 2.0 g maghemite was added to the solution to synthesize 5.0 wt% Pd/maghemite catalyst. In the case of 5.0 wt% Pt- containing catalyst preparation, 0.21 g H_2PtCl_6 was added to 2.0 g maghemite, and 1 mL hydrazine hydrate was also used. The alcoholic dispersion of the precious metal and maghemite was sonicated for 2 min by using the tip homogenizer (20 kHz, 78 W). Pd or Pt was deposited onto the magnetic nanopowder solid. The catalysts were then removed from the cleared and transparent alcoholic phase with a neodymium magnet, washed with patosolv, and dried at 105 °C overnight. A bimetallic catalyst (Pd-Pt/maghemite) with 4.5 wt% Pd and 0.5 wt% Pt was also prepared as described above.

2.4. Catalytic performance tests

The catalytic hydrogenation of 2,4-dinitrotoluene (DNT) was carried out in a Büchi Uster Picoclave reactor (200 mL stainless steel vessel with heating jacket). The pressure of H_2 was kept at 20 bar, and the reaction mixture was kept at 303, 313, 323 and 333 K. Sampling was carried out after 5, 10, 15, 20, 30, 40, 60, 120, 180, and 240 min on reaction stream. The initial concentration of DNT was 0.05 mol L^{-1} in methanol, and 150 mL DNT solution and 0.1 g catalyst were applied during the tests. The formed by-products and reaction intermediates were identified by using a JMS-T200GC AccuTOF GCx-plus chromatograph and a JEOL JMS-T200GC mass spectrometer. For the GC measurements, ZB-1MS column (30 m × 0.25 mm, 0.25 μm) was used. The collected data were analysed and detected molecular species were assigned by using "NIST library search", "Molecular ion search", "Exact Mass Analysis of Molecular Ion", "Isotopic Pattern Analysis" and "EI Fragment Ion Analysis". TDA formation was followed by using an Agilent 7890A gas chromatograph coupled with Agilent 5975C Mass Selective detector. To determine the formed products, analytical standards (2,4-dinitrotoluene, 2,4-diaminotolune, DNT, 2-methyl-5-nitroaniline, 2-methyl-3-nitroaniline, 4-methyl-3-nitroaniline, 4-methyl-2-nitroaniline, Sigma Aldrich Ltd.) have been used.

The activity and selectivity (towards TDA) of the catalysts were determined by calculating the conversion (X, %) of DNT and the TDA yield (Y, %) based on the following Eqs. (1) and (2), respectively:

$$X\% = \frac{consumed\ \boldsymbol{n}_{DNT}}{initial\ \boldsymbol{n}_{DNT}} \bullet 100 \quad (1)$$

$$Y\% = \frac{\boldsymbol{n}_{formed\ TDA}}{\boldsymbol{n}_{theoretical\ TDA}} \bullet 100 \quad (2)$$

Kinetic measuremetns on the studied catalytic reaction in the batch reactor system used were conducted based on initial rates estimation aiming to determine the reaction orders with respect to DNT and H_2. Towards this goal, the initial concentration of DNT ($c_{DNT,0}$) was varied (25, 30 and 40 mmol/L) at constant P_{H2} of 20 bar, while the total pressure of H_2 (P_{H2}) was varied (10, 20, 30 and 40 bar) at constant $c_{DNT,0}$ = 50 mmol/L for the Pd/maghemite catalytic system. The DNT concentration decay after the first 2 min was used to estimate the initial rate of reaction (v_0) by the following Eq. (3):

$$v_0 = -\frac{d[DNT]}{dt} \quad (3)$$

The initial rate (mmol/L s^{-1}) of reaction can be expressed by Eq. (4):

$$v_0 = k_{eff}[DNT]^{\alpha}[H_2]^{\beta} \quad (4)$$

The apparent reaction orders with respect to DNT (α) and H_2 (β) were determined by the linear fit of the $lgc_{DNT,\,0}$ vs. lgv_o relationship at $P = 20$ bar and $lgc_{DNT,\,0}$ vs. lgv_o at $c_{DNT,0}$ = 50 mmol/L using the logarithmic form of Eq. (4):

$$lgv_0 = lgk_{eff} + \alpha lgc_{DNT,0} + \beta lgp_{H2} \quad (5)$$

where, k_{eff} is the effective rate constant ($T = 303$ K).

3. Results and discussion

3.1. Characterization of the nanopowder maghemite

The magnetic catalyst support was examined by HRTEM, and the γ-Fe_2O_3 nanoparticles are clearly visible (Fig. S2, A). The nanopowder is

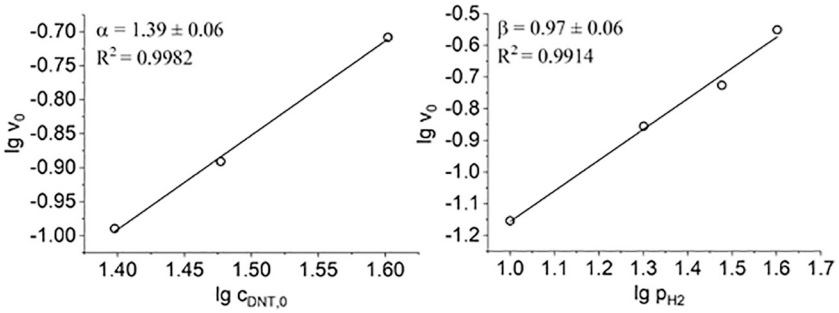

Fig. 1. The logarithm of the initial rate (lgv_0) of DNT hydrogenation as a function of the logarithm of the initial concentration of the DNT ($lg\ c_{DNT,0}$, left graph) and total pressure of H_2 ($lg\ p_{H2,0}$, right graph) at 303 K using the prepared palladium maghemite catalysts.

highly dispersed given the average particle size of 22.0 ± 6.6 nm (Fig. S2, B). The FTIR results indicates that the nanopowder contains carbon as well (Fig. S2, C). The presence of carbon was confirmed by the appearance of the symmetric and asymmetric vibrational bands of the C—H stretching at 2892 and 2835 cm^{-1}. Another IR band at 1631 cm^{-1} also shows the presence of carbon as it can be assigned to the stretching of the C=C bonds. Carbon remained in the sample as a product of the combustion of polyethylene glycol. The exact carbon content was measured by CHNS elemental analysis, and it was found that the sample contained 2.83 wt% carbon. The magnetic nanopowder contains hematite as well (6.8 wt%) next to the main maghemite phase (Fig. S2, D).

Powder XRD measurements were carried out to clarify the phase composition of the magnetic support. After the sonochemical treatment, the PEG-based dispersion was filtered and washed with distilled water and dried at room temperature in vacuum overnight. Based on the diffractogram of this sample, goethite (α-FeO(OH), 10.7 wt%), ferrihydrite ($Fe^{3+}{}_{10}O_{14}(OH)_2$, 22.1 wt%), and PEG (67.2 wt%) were identified (Fig. S3). Based on this, it can be concluded that during the ultrasonication the iron(III) citrate reacted with polyol forming iron oxyhydroxide species which transformed through dehydration/dehydroxylation processes to maghemite and hematite during combustion.

3.2. Characterization of the palladium, platinum, and Pd—Pt maghemite-supported catalysts

BET surface area analysis was carried out for the maghemite-supported catalysts and the support alone. The Pt/maghemite system had the smallest surface area, ca. 10.1 m^2/g, followed by the bimetallic system, ca. 19.2 m^2/g. The Pd/maghemite catalyst had a surface area of 23.1 m^2/g which is more than double compared to the Pt/maghemite catalyst. The specific surface area of the catalyst support alone is 41.7 m^2/g.

The morphology of the solid particles of catalysts has been studied by using HRTEM (Fig. S4, A, C and E). The individual maghemite nanoparticles formed aggregates (ca. 100–150 nm). The Pd and Pt nanoparticles were indistinguishable from the support particles on the HRTEM images. However, the powder XRD results confirmed that reduction of platinum and palladium ions was efficient since the samples contain pure metallic phases. On the X-ray diffractogram of the Pd/maghemite system, Pd(111) and Pd(200) lines can be identified at 40.3° and 46.4° 2theta, respectively (Fig. S4, B and Fig. S5). In the case of Pt catalyst, the Pt(111), Pt(200), and Pt(220) lines were detected, which indicates the presence of elemental platinum (Fig. S4, D and Fig. S6). The presence of the precious metals was detectable in the bimetallic Pd-Pt/maghemite catalyst also (Fig. S4, F and Fig. S7). The average size of the Pd and Pt nanoparticles was 4.6 and 7.4 nm, respectively, based on the XRD results and using the Scherrer equation.

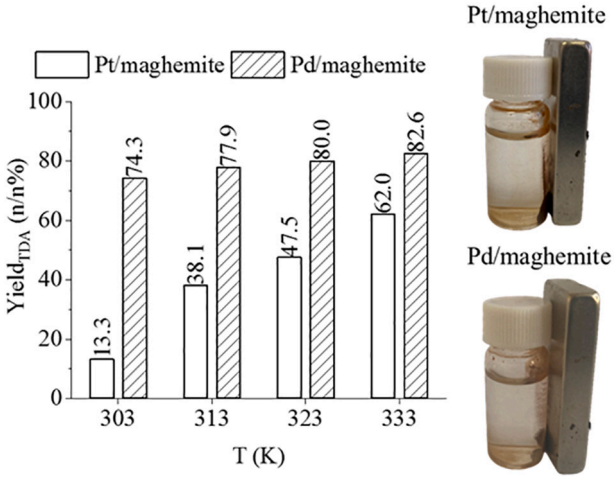

Fig. 2. TDA yields in the 303–333 K range in the case of Pt/maghemite and Pd/maghemite catalysts, and their separation from the reaction medium by using magnetic field.

3.3. Comparison of the catalytic activity of the monometallic maghemite-supported catalysts

The maghemite support alone showed a DNT conversion as high as 77.6% at 333 K, while the TDA yield was 30.5% after 240 min of reaction (Fig. S8). However, due to the low TDA yield, adding a precious metal to the system is essential. The apparent reaction order with respect to each of the reactants and the rate equation of reaction was determined experimentally. The reaction order with respect to DNT (α) and H_2 (β) were determined according to the linear fitting shown in Fig. 1.

A fractional reaction order of ~1.4 is obtained, while the reaction order parameter with respect to hydrogen can be considered as unity (0.97 ± 0.06), meaning a first order kineticsat the studied experimental conditions. The derived effective rate constant (Eq. (4)) of the Pd/maghemite system was found to be in the range of 6.4×10^{-5} and 3.3×10^{-5} ($mmol^{-0.4}\ L^{-0.4}\ bar^{-1}\ s^{-1}$). The apparent reaction order with respect to H_2 (β) is significantly lower in the case of supported Pt (0.55 ± 0.05, Fig. S9) than Pd catalyst (0.97 ± 0.06) which might suggest some strong interactions of H_2 with the catalyst surface, thus leading to high chemical adsorption rates [33].

In the case of Pd/maghemite catalyst, TDA yield was not changed significantly with the reaction temperature, where 30 K difference in temperature resulted only in ~8% improvement in the yield. The maximum TDA yield was 82.6% and it was achieved by using the Pd catalyst at 333 K and 20 bar hydrogen pressure (Fig. 2). The supported platinum catalyst provided only 62.0% yield. However, both catalysts can be easily separated from the reaction medium by magnet (Fig. 2).

A higher TDA yield was achieved by the Pd/maghemite catalyst, and

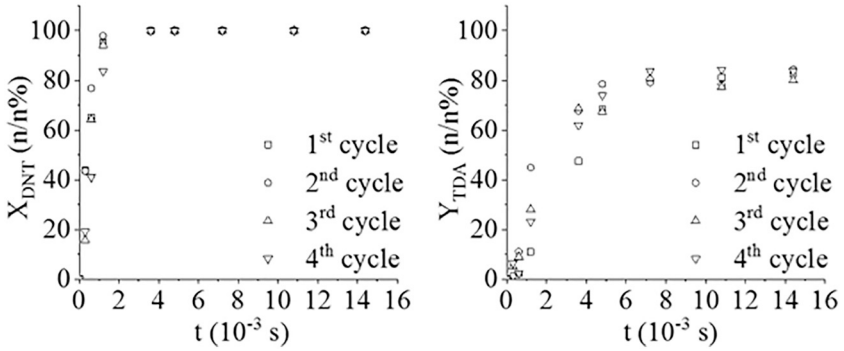

Fig. 3. Reuse tests of the synthesized Pd/maghemite catalyst. DNT conversions and TDA yields vs. hydrogenation time measured at 333 K in four cycles.

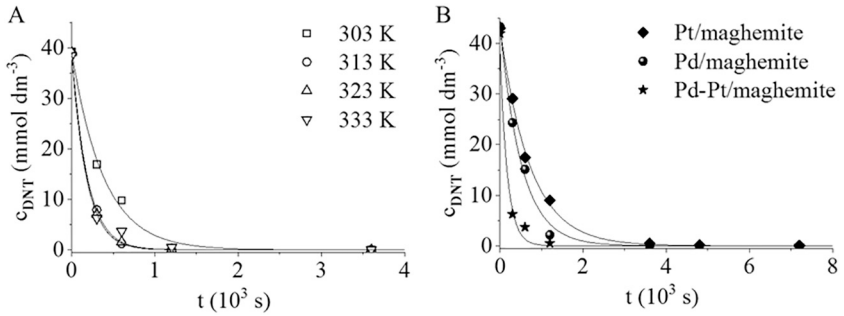

Fig. 4. 2,4-dinitrotoluene (DNT) conversion vs. hydrogenation time at four different temperatures (303−333*K*) by using the Pd-Pt/maghemite bimetallic catalyst (A), and comparison of the two monometallic and bimetallic catalysts at 333 K (B).

thus, this was applied in the reuse tests (Fig. 3). The DNT conversion was stable and did not decreased significantly even after four cycles (Fig. 3). The corresponding TDA yields remained above 80% during the tests (Fig. 3).

Two intermediates were identified during the reaction, 4-amino-2-nitrotoluene (4A2NT) and 2-amino-4-nitrotoluene (2A4NT), which are the semi-hydrogenated species of DNT. The less active Pt/maghemite sample was not able to convert completely the intermediates to TDA (Fig. S10, A, B), while the Pd containing catalyst was successfully achieved this within a reasonable time (Fig. S10, C, D).

Various by-products have been formed during the hydrogenation, and these were identified by using isotopic pattern analysis. Condensed derivatives of DNT and TDA such as *p*-tolualdehyde-2,4-dinitro-phenylhydrazone ($C_{14}H_{12}N_4O_4$) and 2-methyl-1-[(2-methyl-4-nitrophenyl)-NNO-azoxy]-4-nitrobenzene ($C_{14}H_{12}N_4O_5$) and others have been formed (Table S1).

3.4. Catalytic activity of bimetallic maghemite-supported catalysts

Although both precious metals deposited on maghemite support were highly active, a bimetallic catalyst was also prepared (4.5 wt% Pd and 0.5 wt% Pt) and tested under the same reaction conditions as the monometallic ones. The rates of hydrogenation at 303 and 313 K were similar (Fig. 4 A), and the reaction rate constant (*k*) values estimated were 5.4×10^{-3} s^{-1} and 5.7×10^{-3} $mmol^{-0.4}$ $L^{-0.4}$ bar^{-1} s^{-1}, respectively. The reaction rate constants were very similar (1.8×10^{-3} s^{-1} and 1.9×10^{-3} $mmol^{-0.4}$ $L^{-0.4}$ bar^{-1} s^{-1}) at 333 K when the monometallic Pd and Pt catalysts were used, but a significant increase of k value ($5.7 \times 10^{-3} \pm 4.0 \bullet 10^{-5}$ $mmol^{-0.4}$ $L^{-0.4}$ bar^{-1} s^{-1}) was achieved (~ 3 times) with the bimetallic catalyst (Fig. 4 B). After 10 min of hydrogenation, the DNT conversion was 90.4% at 333 K compared to 65.0% in the case of Pd/maghemite. The TDA yield reached 86.8% at 333 K with the Pd-Pt/maghemite catalyst, which is slightly higher compared to the Pd/maghemite system (82.6% at 333 K).

4. Conclusions

Nanosized maghemite powder was synthesized by using a recently developed combined combustion and sonochemical methods. By ultrasonic treatment, iron oxyhydroxide species formed were transformed through dehydration/dehydroxylation processes to maghemite and hematite phases during the combustion step. The prepared magnetic nanopowder was used as catalyst support. Monometallic palladium and platinum maghemite-supported catalysts and their bimetallic Pd—Pt counterpart were successfully synthesized after using a fast, relatively easy, and efficient catalyst preparation method, which does not include post-treatments. Their catalytic activity for the 2,4-toluenediamine (TDA) synthesis was tested, and in each case full conversion of 2,4-dinitrotoluene (DNT) was achieved after 60 min. However, the TDA yield was higher when Pd/maghemite (82.6% at 333 K) catalyst was used compared to the Pt/maghemite case (62.0% at 333 K). By combining the two precious metals, a more active bimetallic catalyst was developed and 90.4% of DNT conversion was reached after 10 min. Furthermore, after 30 min of reaction, full conversion of DNT was obtained over the bimetallic catalyst, while the monometallic catalysts exhibited lower conversion rates at the same reaction time of 30 min. In the present work, three maghemite-supported magnetic catalysts were successfully produced in an easy and fast synthetic route, and their catalytic activity was remarkable. In addition, these maghemite-based catalysts are easily separable from the reaction medium due to their magnetic behaviour.

Declaration of Competing Interest

On behalf of all authors, the corresponding author states that there is no conflict of interest.

Acknowledgements

This research was supported by the European Union and the

Hungarian State, co-financed by the European Regional Development Fund in the framework of the GINOP-2.3.4-15-2016-00004 project aimed to promote the cooperation between higher education and the industry. We also thank Angelos M. Efstathiou for his insightful comments and corrections, which significantly improved the quality of the manuscript.

Appendix A. Supplementary data

Supplementary data to this article can be found online at https://doi.org/10.1016/j.catcom.2021.106342.

References

[1] G. Neri, M.G. Musolino, C. Milone, et al., Mechanism of 2,4-dinitrotoluene hydrogenation over Pd/C, J. Mol. Catal. A Chem. 95 (1995) 235–241, https://doi.org/10.1016/1381-1169(94)00002-6.
[2] G. Neri, M.G. Musolino, C. Milone, et al., Particle size effect in the catalytic hydrogenation of 2,4-dinitrotoluene over Pd/C catalysts, Appl. Catal. A Gen. 208 (2001) 307–316, https://doi.org/10.1016/S0926-860X(00)00717-1.
[3] E. Auer, M. Gross, P. Panster, K. Takemoto, Supported indium catalysts - a novel catalytic system for the synthesis of toluenediamine, Catal. Today 65 (2001) 31–37, https://doi.org/10.1016/S0920-5861(00)00542-3.
[4] F. Pinna, M. Selva, M. Signoretto, et al., Pd-Fe/SiO2 catalysts in the hydrogenation of 2, 4-Dinitrotoluene, J. Catal. 150 (1994) 356–367, https://doi.org/10.1006/jcat.1994.1354.
[5] A. Benedetti, G. Fagherazzi, F. Pinna, et al., The influence of a second metal component (Cu, Sn, Fe) on Pd/SiO2 activity in the hydrogenation of 2,4-dinitrotoluene, Catal. Lett. 10 (1991) 215–223, https://doi.org/10.1007/BF00772074.
[6] E.J. Molga, K.R. Westerterp, Kinetics of the hydrogenation of 2,4-dinitrotoluene over a palladium on alumina catalyst, Chem. Eng. Sci. 47 (1992) 1733–1749, https://doi.org/10.1016/0009-2509(92)85021-3.
[7] M.V. Rajashekharam, D.D. Nikalje, R. Jaganathan, R.V. Chaudhari, Hydrogenation of 2,4-dinitrotoluene using a Pd/Al2O3 catalyst in a slurry reactor: a molecular level approach to kinetic modeling and nonisothermal effects, Ind. Eng. Chem. Res. 36 (1997) 592–604, https://doi.org/10.1021/ie960365l.
[8] X. Ren, J. Li, S. Wang, et al., Preparation and catalytic performance of ZrO_2 -supported Pt single-atom and cluster catalyst for hydrogenation of 2,4-dinitrotoluene to 2,4-toluenediamine, J. Chem. Technol. Biotechnol. 95 (2020) 1675–1682, https://doi.org/10.1002/jctb.6359.
[9] H.J. Janssen, A.J. Kruithof, G.J. Steghuis, K.R. Westerterp, Kinetics of the catalytic hydrogenation of 2,4-Dinitrotoluene. 2. Modeling of the reaction rates and catalyst activity, Ind. Eng. Chem. Res. 29 (1990) 1822–1829, https://doi.org/10.1021/ie00105a013.
[10] M.G. Musolino, C. Milone, G. Neri, et al., Selective catalytic hydrogenation of 2,4-dinitrotoluene to nitroarylhydroxylamines on supported metal catalysts, Stud. Surf. Sci. Catal. 108 (1997) 239–246, https://doi.org/10.1016/s0167-2991(97)80910-x.
[11] R.V. Malyala, R.V. Chaudhari, Hydrogenation of 2,4-dinitrotoluene using a supported Ni catalyst: reaction kinetics and semibatch slurry reactor modeling, Ind. Eng. Chem. Res. 38 (1999) 906–915, https://doi.org/10.1021/ie980423y.
[12] R.B.N. Baig, R.S. Varma, Magnetically retrievable catalysts for organic synthesis, Chem. Commun. 49 (2013) 752–770, https://doi.org/10.1039/c2cc35663e.
[13] P. Ghosh, A. Mandal, R. Subba, γ-Maghemite-silica nanocomposite: a green catalyst for diverse aromatic N-heterocycles, Catal. Commun. 41 (2013) 146–152, https://doi.org/10.1016/j.catcom.2013.06.026.
[14] J.O. Damas, S.B. Moscardini, L.R. Oliveira, et al., Effect of silica coating on the catalytic activity of maghemite nanoparticles impregnated into mesoporous silica matrix, Mater. Chem. Phys. 225 (2019) 145–152, https://doi.org/10.1016/j.matchemphys.2018.12.051.
[15] H. Cui, W. Ren, Low temperature and size controlled synthesis of monodispersed γ-Fe2O3 nanoparticles by an epoxide assisted sol-gel route, J. Sol-Gel Sci. Technol. 47 (2008) 81–84, https://doi.org/10.1007/s10971-008-1695-2.
[16] O.M. Lemine, K. Omri, M. Iglesias, et al., γ-Fe2O3by sol-gel with large nanoparticles size for magnetic hyperthermia application, J. Alloys Compd. 607 (2014) 125–131, https://doi.org/10.1016/j.jallcom.2014.04.002.
[17] J. Vidal-Vidal, J. Rivas, M.A. López-Quintela, Synthesis of monodisperse maghemite nanoparticles by the microemulsion method, Colloids Surf. A Physicochem. Eng. Asp. 288 (2006) 44–51, https://doi.org/10.1016/j.colsurfa.2006.04.027.
[18] A.B. Chin, I.I. Yaacob, Synthesis and characterization of magnetic iron oxide nanoparticles via w/o microemulsion and Massart's procedure, J. Mater. Process. Technol. 191 (2007) 235–237, https://doi.org/10.1016/j.jmatprotec.2007.03.011.
[19] E. Darezereshki, Synthesis of maghemite (γ-Fe2O3) nanoparticles by wet chemical method at room temperature, Mater. Lett. 64 (2010) 1471–1472, https://doi.org/10.1016/j.matlet.2010.03.064.
[20] M. Nazari, N. Ghasemi, H. Maddah, M.M. Motlagh, Synthesis and characterization of maghemite nanopowders by chemical precipitation method, J. Nanostruct. Chem. 4 (2014) 1–5, https://doi.org/10.1007/s40097-014-0099-9.
[21] O. Horner, S. Neveu, S. De Montredon, et al., Hydrothermal synthesis of large maghemite nanoparticles: influence of the pH on the particle size, J. Nanopart. Res. 11 (2009) 1247–1250, https://doi.org/10.1007/s11051-008-9582-x.
[22] G. Salazar-Alvarez, M. Muhammed, A.A. Zagorodni, Novel flow injection synthesis of iron oxide nanoparticles with narrow size distribution, Chem. Eng. Sci. 61 (2006) 4625–4633, https://doi.org/10.1016/j.ces.2006.02.032.
[23] R. Ianoş, A. Tăculescu, C. Păcurariu, I. Lazău, Solution combustion synthesis and characterization of magnetite, Fe 3O 4, nanopowders, J. Am. Ceram. Soc. 95 (2012) 2236–2240, https://doi.org/10.1111/j.1551-2916.2012.05159.x.
[24] Á. Prekob, Muránszky Gábor, I. Kocserha, et al., Sonochemical deposition of palladium nanoparticles onto the surface of N-doped carbon nanotubes: a simplified one-step catalyst production method, Catal. Lett. 3 (2020) 505–513, https://doi.org/10.1007/s10562-019-03074-1.
[25] V. Hajdu, Á. Prekob, G. Muránszky, et al., Catalytic activity of maghemite supported palladium catalyst in nitrobenzene hydrogenation, React. Kinet. Mech. Catal. 129 (2020) 107–116, https://doi.org/10.1007/s11144-019-01719-1.
[26] K.S. Suslick, Sonochemistry, in: In: Kirk-Othmer Encyclopedia of Chemical Technology, John Wiley & Sons, Inc, Hoboken, NJ, USA, 2000.
[27] Q.I.U. Xiao Feng, Z.H.U. Jun Jie, Synthesis of palladium nanoparticles by a Sonochemical method, Chinese J. Inorg. Chem. 19 (2003) 766–770.
[28] X.F. Qiu, J.J. Zhu, H.Y. Chen, Controllable synthesis of nanocrystalline gold assembled whiskery structures via sonochemical route, J. Cryst. Growth 257 (2003) 378–383, https://doi.org/10.1016/S0022-0248(03)01467-2.
[29] Y. Yu, Q.Y. Zhang, X.G. Li, Reduction process of transition metal ions by zinc powder to prepare transition metal nanopowder, Acta Phys. -Chim. Sin. 19 (2003) 436–440, https://doi.org/10.3866/pku.whxb20030512.
[30] S.H. Wu, D.H. Chen, Synthesis and characterization of nickel nanoparticles by hydrazine reduction in ethylene glycol, J. Colloid Interface Sci. 259 (2003) 282–286, https://doi.org/10.1016/S0021-9797(02)00135-2.
[31] C. Kan, W. Cai, C. Li, et al., Ultrasonic synthesis and optical properties of au/Pd bimetallic nanoparticles in ethylene glycol, J. Phys. D. Appl. Phys. 36 (2003) 1609–1614, https://doi.org/10.1088/0022-3727/36/13/328.
[32] Q. Li, H. Li, V.G. Pol, et al., Sonochemical synthesis, structural and magnetic properties of air-stable Fe/Co alloy nanoparticles, New J. Chem. 27 (2003) 1194–1199, https://doi.org/10.1039/b302136j.
[33] Costas L. Constantinou, Costas N. Costa, Angelos M. Efstathiou, Catalytic removal of nitrates from waters, Catal. Today 151 (2010) 190–194, https://doi.org/10.1016/j.cattod.2010.02.019.